Title

A robust and quantitative method for tracking liposome contents after intravenous administration

Journal

Journal of Controlled Release, 176(1)

ISSN

0168-3659

Authors

Kohli, Aditya G
Kieler-Ferguson, Heidi M
Chan, Darren
et al.

Publication Date

2014-02-01

DOI

10.1016/j.jconrel.2013.12.014

Peer reviewed

Published in final edited form as:
J Control Release. 2014 February 28; 176: 86–93. doi:10.1016/j.jconrel.2013.12.014.

A robust and quantitative method for tracking liposome contents after intravenous administration

Aditya G. Kohli[#1,2], **Heidi M. Kieler-Ferguson**[#3], **Darren Chan**[2], and **Francis C. Szoka**[1,2]

[1]UC-Berkeley-UCSF Graduate Program in Bioengineering, University of California Berkeley, Berkeley, CA 94720

[2]Department of Bioengineering, Therapeutic Sciences and Pharmaceutical Chemistry, University of California San Francisco, San Francisco, CA 94143.

[3]Department of Chemistry, University of California, Berkeley, CA 94720.

[#] These authors contributed equally to this work.

Abstract

We introduce a method for tracking the rate and extent of delivery of liposome contents *in vivo* based on encapsulation of 4-methylumbelliferyl phosphate (MU-P), a profluorophore of 4-methylumbelliferone (MU). MU-P is rapidly dephosphorylated by endogenous phosphatases *in vivo* to form MU after leakage from the liposome. The change in fluorescence spectra when MU-P is converted to MU allows for quantification of entrapped (MU-P) and released (MU) liposome contents by fluorescence or by a sensitive high performance liquid chromatography assay. We define the "cellular availability" of an agent encapsulated in a liposome as the ratio of the amount of released agent in the tissue to the total amount of agent in the tissue; this parameter quantifies the fraction of drug available for therapy. The advantage of this method over existing technologies is the ability to decouple the signals of entrapped and released liposome contents. We validate this method by tracking the circulation and tissue distribution of MU-P loaded liposomes after intravenous administration. We use this assay to compare the cellular availability of liposomes composed of engineered phosphocholine lipids with covalently attached cholesterol, sterol-modified lipids (SML), to liposomes composed of conventional phospholipids and cholesterol. The SML liposomes have similar pharmacokinetic and biodistribution patterns as conventional phospholipid-cholesterol liposomes but a slower rate of contents delivery into the tissue. Thus, MU-P enables the tracking of the rate and extent of liposome contents release in tissues and

Corresponding Author Francis C. Szoka szoka@cgl.ucsf.edu School of Pharmacy, University of California, 513 Parnassus Ave., Box 0912, San Francisco, CA, 94143, USA 415-476-3895 .

Conflict of Interest Dr. Szoka declares a conflict of interest due to patent applications concerning the SML filed by the University of California and due to his involvement in a liposome company. The other authors declare no conflict of interest.

Contributions A.G.K., H.M.KF and F.C.S conceived and designed the experiments. A.G.K. and H.M.KF performed experiments. S.K. and D.C. conducted animal experiments. A.G.K and H.M.KF analyzed the data. A.G.K., H.M.KF and F.C.S. wrote the paper.

should facilitate a better understanding of the pharmacodynamics of liposome-encapsulated drugs in animals.

Keywords

Liposomes; 4-methylumbelliferone; sterol-modified lipids; drug release

1. Introduction

A quantitative understanding of where and when liposome encapsulated agents are released in vivo is critical in the rational design of liposomes for drug therapy. While liposomes may accumulate at the target site, only drug released from the liposome, “cellular available” drug, has biological activity. Drug trapped in the liposome has little therapeutic consequence as illustrated by the poor performance of liposome-encapsulated cis-platinum in humans [1]. Liposomal therapeutics should be optimized to release their payload over a timescale defined by the pharmacology of the payload and the biology of the therapeutic target. While there are several methods to quantify liposome pharmacokinetics and assess accumulation of liposomes and payload in target tissues, few approaches can differentiate the signals of the encapsulated and released payload. This paucity of experimental approaches to measure cellular availability has limited the optimization of liposomes for drug delivery.

Microscopic, radioactive, magnetic resonance, and fluorescent tracers have been the principal tools for tracking liposomes *in vivo* [2]. Microscopy studies have demonstrated the cellular compartmentalization of liposomes and established the reticuloendothelial system (RES) as a mediator of liposome clearance [3]. Encapsulated radioactive tracers or iodinated lipid markers have confirmed that the liver, spleen, bone marrow, and tumor are the primary sites of liposome accumulation *in vivo* [4-8]. However, these studies have provided little insight into the release of liposomal payloads in tissues. Results that rely on bilayer embedded or encapsulated fluorescent tracers such as carbocyanine dyes [9] or fluorescence resonance energy transfer (FRET) pairs [10], can be confounded due to exchange of the probe into lipoproteins and cell membranes [11]. Encapsulation of self-quenching fluorescent compounds, such as carboxyfluorescein (CF) [12] and doxorubicin [13-15], or fluorophore-quencher pairs [16] is useful for measuring entrapped and released contents in plasma samples, but physical and chemical tissue homogenization steps that disrupt the lipid bilayer limit the ability of these probes to report on the cellular availability.

A small number of studies have focused on decoupling the signals of entrapped and released liposome contents in tissues [17-20]. Laginha and colleagues approximated the fraction of leaked doxorubicin by measuring doxorubicin in tumor nuclei and assuming that all released drug is bound to DNA [18]. However, this approach is specific for the *in vivo* disposition of doxorubicin crystallized in the liposome and reliant on the drug’s interactions with DNA. The Baldeschwieler group used perturbed angular correlation spectroscopy to quantify entrapped and released ^{111}In [20]. While safe and broadly applicable, this method is limited by its sensitivity. Previously, our group quantified the cellular availability of liposomal contents using a dual radiolabeled reporter system: [^{51}Cr]EDTA and [^{22}Na] [21]**.** While

[^{22}Na] is exported by the cell, [^{51}Cr] is not, and the ratio of the two components measures the liposome cellular availability. While promising, this method has proven to be too complicated for widespread use. Taken together, these studies show that there is a need for quantitative methods to distinguish between entrapped and released liposomal contents in tissues.

We developed a broadly applicable and sensitive method for tracking liposome cellular availability *in vivo* in which 4-methylumbelliferyl phosphate (MU-P), a water soluble profluorophore of 4-methylumbelliferone (MU) is encapsulated in liposomes (Figure 1) [22]. Release of this compound from liposomes *in vivo* results in its rapid dephosphorylation to form MU (Figure 2A); MU, MU metabolites and MU-P can then be quantified by fluorescence or by high-performance liquid chromatography (HPLC). This method allows researchers to obtain a new level of granularity when investigating liposome biodistribution.

We use this method to determine if restricting the transfer of cholesterol out of the liposome bilayer reduces the release of liposome contents in tissues. We used liposomes composed of sterol-modified lipids (SML), in which cholesterol is covalently attached to the phosphoglycerol backbone in place of an acyl chain [23,24]. We compare pharmacokinetics, biodistribution, and cellular availability of SML to that of liposomes composed of conventional phospholipids and cholesterol (CPL) and find that while SML and CPL have similar pharmacokinetic profiles; MU-P encapsulated in SML has greater accumulation and longer persistence in the liver and spleen. This indicates that at certain chain lengths SML release contents slower than CPL.

2. Materials and Methods

2.1 Lipids

1,2-dilauroyl-*sn*-glycero-3-phosphocholine (C_{12} PC), 1,2-dimyristoyl-*sn*-glycero-3-phosphocholine (C_{14} PC), 1,2-dipalmitoyl-*sn*-glycero-3-phosphocholine (C_{16} PC), L-α-phosphatidylcholine hydrogenated (C_{18} PC), 1,2-diarachidoyl-*sn*-glycero-3-phosphocholine (C_{20} PC), 1,2-dibehenoyl-*sn*-glycero-3-phosphocholine (C_{22} PC) 1-palmitoyl-2-oleoyl-*sn*glycero-3-phosphocholine ($C_{18:1}$ PC), 1,2-dioleoyl-*sn*-glycero-3-phosphocholine (DOPC), 1,2-dicholesterylhemisuccinoyl-*sn*-glycero-3-phosphocholine (DCHEMSPC), 1-lauroyl-2-cholesterylhemisuccinoyl-*sn*-glycero-3-phosphocholine (C_{12} SML), 1-myristoyl-2-cholesterylhemisuccinoyl-*sn*-glycero-3-phosphocholine (C_{14} SML), 1-palmitoyl-2-cholesterylhemisuccinoyl-*sn*-glycero-3-phosphocholine (C_{16} SML), 1-stearoyl-2-cholesterylhemisuccinoyl-*sn*-glycero-3-phosphocholine (C_{18} SML), 1-rachidoyl-2-cholesterylhemisuccinoyl-*sn*-glycero-3-phosphocholine (C_{20} SML), 1-behenoyl-2-cholesterylhemisuccinoyl-*sn*-glycero-3-phosphocholine (C_{22} SML) 1-oleoyl-2-cholesterylhemisuccinoyl-*sn*-glycero-3-phosphocholine (C18:1 SML), 1,2-distearoyl-*sn* glycero-3-phosphoethanolamine-N-[methoxy(polyethylene glycol)-2000] (DSPE-PEG), and cholesterol were purchased from Avanti Polar Lipids, kindly donated by Dr. Zhaohua Huang, or synthesized as previously described [23,24].

2.2 Materials and Instrumentation

MU, MU-P, MU-S, MU-G and 7-hydroxycoumarin were obtained from Sigma. Solvents were removed under reduced pressure using a rotary evaporator. Average liposome diameter and zeta potential measurements were determined using the Zetasizer Nano ZS (Malvern Instruments). Fluorescence spectroscopy was measured on a FluoroLog-3 spectrofluorimeter (Horiba Jobin Yvon) equipped with a temperature-controlled stage (LFI-3751) or using a Tecan Infinite 4300 (Tecan Group Ltd). Data acquisition was done through FluorEssence software (Horiba Scientific). High-pressure liquid chromatography (HPLC) was performed on an Agilent 1100 HPLC (Agilent).

2.3 Serum Conversion of MU Prodrugs

MU-P or MU-S were dissolved in phosphate buffered saline (2.7mM KCl, 1.5mM KH_2PO_4, 136.9mM NaCl, 8.9mM Na_2HPO_4, pH 7.4; PBS) and incubated with 50% mouse serum at 37°C. Prodrug conversion to MU was monitored by measuring MU fluorescence every 5 minutes over 12 hours. Data was fit to a Michaelis-Menten model using GraphPad Prism.

2.4 Liposomes for Contents Leakage

Lipids were dissolved in chloroform, dried to form a thin film, and placed under high vacuum overnight. Lipid mixtures included Diacyl:Chol:PEG (55:40:5), Diacyl:SML:PEG (55:40:5), SML:PEG (95:5), and DiChems:Diacyl:PEG (20:75:5) with acyl chain lengths of C_{12}-C_{22}. The films were re-hydrated with 1 mL CF (50 mM) or 1 mL MU-P (300 mM) in Hepes buffered saline (10 mM Hepes, 140 mM NaCl, pH 7.4; HBS) at 60°C and vortexed to obtain a lipid concentration of 5 mM. The liposomes were sonicated at 60°C until opalescent (~10 min) and extruded through 200 nm and 100 nm polycarbonate membranes at 60°C. Liposomes were purified on a Sephadex G-25 size exclusion column. In order to quantify CF release from liposomes, CF fluorescence (excitation 492 nm, emission 517 nm) was measured before and after disrupting the lipid membrane with $C_{12}E_{10}$ surfactant. MU-P fluorescence was measured by diluting liposomes into HBS containing calf intestinal phosphatase (New England BioLabs). MU-P outside the liposomes is converted to MU, while MU-P inside the liposomes remains phosphorylated. The fluorescence of MU was measured (excitation 360, emission 449) before and after liposome lysis. The liposome samples were incubated at 37°C in the presence or absence of 30% fetal bovine serum (FBS) for 30 days. Sodium azide (0.05%) was added to limit bacterial growth.

2.5 Liposomes for Animal Studies

Liposomes that were used in animals were prepared by an ethanol injection method followed by extrusion. Lipids dissolved in chloroform were dried to form a thin film and placed under high vacuum overnight. Lipids were dissolved in 200 μL ethanol, heated to 50°C and injected into a stirring 1.8 mL solution of 300 mM MU-P in HBS. After 20 minutes, the liposomes were extruded through 200 nm and 100 nm polycarbonate membranes and dialyzed against HBS with frequent buffer exchange. Before injection into animals, liposomes were separated from non-encapsulated MU-P on a Sephadex G-25 size exclusion column and sterile filtered through 0.2 micron sterile filters.

2.6 Fluorescent Anisotropy

Lipids were dissolved in chloroform, dried to form a thin film, and placed under high vacuum overnight. The films were hydrated with PBS at 65°C and vortexed to obtain a lipid concentration of 5 mM. The liposomes were sonicated at 65°C until opalescent and then extruded through 200 nm and 100 nm polycarbonate membranes at 65°C. Liposomes were diluted 8-fold with PBS and 6 μl of 1,6-diphenyl-1,3,5-hexatriene (DPH, Molecular Probes) in tetrahydrofuran (0.15 mg/ml) was added to the sample. To allow the DPH to integrate into the bilayer, the mixture was incubated at 65°C for 1 hour. Anisotropy measurements were obtained as previously described [25]. Briefly, DPH was excited at 350 nm and the fluorescence detected at 430 nm. With mixing, the liposomes were heated or cooled in 5°C increments from 5–62°C, with a 5–10 minute equilibration between transitions.

2.7 Biodistribution and Pharmacokinetics Studies

All animal experiments were performed in compliance with the NIH guidelines for animal research under a protocol approved by the Committee on Animal Research at the University of California, San Francisco. CD-1 mice were injected via the tail vein with 20 mg/kg MU-P equivalents in a volume of 0.2 mL. For pharmacokinetic studies, blood was collected 10, 20, 60, 180, 1440 and 2880 minutes (3 mice per group) after injection and centrifuged for 10 min at 15,000 g. Serum was collected in a tube with a 1:100 dilution of Phosphatase Inhibitor Cocktail 2 (Sigma). Ten μL of serum was added to 2 mL of HBS along with 10 μL of a 15% $C_{12}E_{10}$ solution. A standard curve was made by titrating MU-P loaded liposomes into the serum from an untreated mouse. MU-P (excitation 320 nm, emission 385 nm), MU (excitation 360 nm, emission 449 nm), and DiD (excitation 644 nm, emission 664 nm) were measured from each serum sample. The data was fit to a two-compartment model using GraphPad Prism. For biodistribution studies, tissues were isolated and flash frozen 3 and 48 hours after injection.

2.8 Biodistribution of MU-P and metabolites by HPLC

Tissues were thawed at room temperature and homogenized by bead beating in a homogenization solution (50% Methanol, 0.1% TFA, 1:100 dilution of Phosphatase Inhibitor Cocktail 2, 1 μg/mL 7-hydroxycoumarin as an internal standard). Homogenized tissues were frozen overnight and sedimented by centrifugation (15,000 g, 15 minutes). The supernatant was passed through a 0.22 μm filter (Fisherbrand, 13mm). Forty μL of the filtered tissue homogenate was injected on a C_8 column (ZORBAX Eclipse XDB-C8 5-Micron) with the following solvent system: Mobile Phase A: 0.1% TFA, Mobile Phase B: 0.1% TFA/MeOH at 1.0 mL/min over a gradient of 10% B to 70% B over 10 minutes with a 5 minute re-equilibration at 40°C and detection at 320 nm. Biodistribution data was extrapolated by fitting peak areas to standard curves of MU, MU-P, and MU-G. All data was normalized to the internal standard.

3. Results

3.1 MU-P Reporter System

MU derivatives are commonly used freagents for determining enzymatic activity of phosphatases (MU-P) and sulfatases (methylumbelliferyl sulfate; MU-S) by fluorescence (Figure 1)[22,26]. The MU profluorophores, MU-P (excitation 320, emission 385) and MUS (excitation 334, emission 370), have shifted fluorescent spectra from MU (excitation 360, emission 449) that allows for independent quantification. We used these common reporter systems to develop an assay to measure liposome contents release (Figure 2A).

We characterized MU-P and MU-S stability in serum in order to choose the optimal profluorophore for encapsulation in liposomes (Figure 2B,C). The kinetics of MU-P conversion to MU (K_m: 0.47 mM, V_{max}: 10.2 nmol/min) were significantly greater than the kinetics of MU-S to MU (K_m: 16.8 mM, V_{max}: 0.32 nmol/min). This may be due to higher levels of phosphatases than sulfatases in serum or due to a difference in enzyme affinity for MU-P and MU-S. We hypothesized that if the lipid bilayer was disrupted, the profluorophore would be released into the tissue environment and rapidly converted to MU. As such, we chose MU-P as the tracer molecule because of its rapid conversion to MU in serum. We further assume that MU-P in the liposome is protected from phosphatase activity. Distinct quantification of MU-P and MU therefore gives a reading of entrapped (MU-P) and released (MU) contents.

3.2 Effects of Acyl Chain Length, Saturation, and Liposome Composition on Membrane Stability

CF (Figure 1) is widely used to measure contents release from liposomes[12], as CF fluorescence is quenched while concentrated in the liposome, but easily quantifiable after release from the liposome. Using the CF reporter system as a benchmark, we first sought to validate our reporter system *in vitro* by establishing a relationship between liposome formulation and stability. CF and MU-P were passively encapsulated into a library of liposome formulations (Figure 3C) and the release of the reporter molecules was monitored by fluorescence in the presence (Figure 3A,B) and absence (Supplementary Figure 1) of serum.

MU-P is more stably encapsulated in liposomes than CF (Figure 3): likely due to the dual negative charge on the phosphate (pKa 7.8 [27]) that prevents the drug from crossing the hydrophobic core of the lipid bilayer. As expected, formulations composed of lipids with long and saturated acyl chains are more stable than those composed of lipids with short or unsaturated acyl chains (Figure 3; Supplementary Table 1).

SML (Δ) encapsulating CF are most stable if they contain lipids with intermediate acyl chain length (C_{16} and C_{18}), and are less stable at both lower and higher chain lengths or when the SML acyl chain is unsaturated (Figure 3A,B; Supplementary Table 1). This “U” shaped stability pattern indicates an optimal SML bilayer packing conformation at intermediate chain lengths, with less stable packing conformations at both higher and lower chain lengths. In contrast, CPL (○) exhibit binary stability: they are highly unstable at chain lengths below C_{16} and show minimal leakage at chain lengths above C_{16} (Figure 3A,B). This dramatic

change in stability is due to tighter membrane packing because of increased hydrophobic interactions at higher chain length. While SML appear more stable than CPL at low chain lengths (C_{12} and C_{14}), they are still relatively unstable, releasing more than 60% of their contents over 14 days. Formulations incorporating DCHEMSPC as a substitute for cholesterol (□) and liposomes containing a mix of di-substituted saturated acyl chains and SML (◇) follow a similar pattern to CPL: they are unstable at low chain lengths but stable at high chain lengths (Supplementary Figure 2).

In contrast to CF, MU-P is stably encapsulated in both SML (Δ) and CPL (○) across chain lengths (Figure 3A,B). This stability highlights the utility of MU-P as a probe to measure contents release from highly unstable liposome formulations that could not be measured using CF (Figure 3A,B, lower left quadrant). Liposomes composed of a mixture of SML and diacyl lipids were highly unstable if they contained acyl chains shorter than C_{18} (Supplementary Figure 2). This reduction in stability may be indicative of heterogeneous packing of the SML and diacyl lipids in the membrane.

3.3 SML and CPL Demonstrate Comparable Membrane Fluidity

To further characterize the membranes of liposomes composed of SML, we measured membrane fluidity using fluorescence anisotropy. A fluorescent probe was incorporated into the liposome membrane and fluidity was deduced by measuring the motility of a fluorophore in the bilayer by anisotropy [28]. Membranes with higher anisotropy values are more rigid while those with lower anisotropy values are more fluid. The SML and the control formulation (C_{16} PC:cholesterol) showed similar anisotropy values over a range of temperatures (Supplementary Figure 3A). As expected, membrane fluidity increases as a function of temperature.

Anisotropy for a typical PC lipid will follow a sigmoidal pattern: high anisotropy values at low temperatures are indicative of the rigid, crystalline state of the lipids. As temperature increases, the lipids undergo a phase transition to a fluid state, indicated by a sharp change in anisotropy (Supplementary Figure 3B). Addition of cholesterol into a membrane eliminates the lipid's natural phase transition and forces the bilayer into a permanent gel-like state that is neither fluid nor rigid. This state is crucial to the maintenance of bilayer stability. The loss in phase transition is reflected on the anisotropy plots (Supplementary Figure 3). SML exhibit no phase transition, which indicates that the SML bilayers are also in a gel-like state. As such, while conjugation of cholesterol to the lipid backbone influences contents release rates, it does not significantly modify the bilayer structure.

3.4 Evaluation of SML and CPL Stability in Circulation by Fluorescence

We compared the pharmacokinetics of SML and CPL after intravenous injection via the tail vein in mice. MU-P was passively encapsulated into liposomes and a far-red fluorescent lipid, $DiIC_{18}$ (DiD), was incorporated into the lipid membrane. This permitted independent tracking of the liposome and its contents. After encapsulation of MU-P, all liposomes studied had similar sizes and zeta potentials (Supplementary Table 2). Serum was collected from mice directly into a tube with phosphatase inhibitor. The liposome contents (MU-P),

released contents (MU), and lipid (DiD) were measured in serum samples using fluorescence as a function of time after injection (Figure 4).

After injection of MU-P containing liposomes, MU could not be detected by fluorescence. After MU-P is released from the liposomes, it is rapidly converted to MU by serum phosphatases and is rapidly eliminated [29]. We assume that the MU-P signal measured in serum was entrapped in liposomes, as free MU-P is also quickly cleared from circulation ($t_{1/2}$: 17 minutes). The MU-P and DiD serum concentrations over time were fit to a two-compartment model (Figure 4, Supplementary Table 2), and the ratio of the total exposure of MU-P to the total exposure of lipid ($AUC_{MU\text{-}P}/AUC_{DiD}$) quantifies how stably the liposomes retain their contents in circulation (Figure 4I).

SML and CPL with acyl chain lengths of C_{16} and C_{18} formed the most stable liposomes (Figure 4A-D), as their $AUC_{MU\text{-}P}/AUC_{DiD}$ ratios approach 1**.** In sharp contrast, liposomes with C_{20} acyl chain lengths or with unsaturated fatty acid tails were relatively unstable in circulation, as demonstrated by the rapid loss of contents signal after injection (Figure 4EH). C_{20} CPL were more stable than C_{20} SML. C_{20} lipids form liposomes with a thicker bilayer than lipids with shorter acyl chains. In this bilayer context, it may be advantageous for cholesterol to be in a free state to adopt its optimal packing conformation. Constraining the cholesterol in the C_{20} SML by covalently attaching it to the headgroup may contribute to the relative instability of the SML.

Taken together, these results highlight the increased serum stability of SML as compared to CPL and validate the MU-P/MU fluorescent reporter system as a method to track liposomes in circulation.

3.5 SML Alter Contents Delivery to the Liver and Spleen

Most current methods for measuring tissue biodistribution of liposomes fail to differentiate between entrapped and released contents, as the liposome membrane is often compromised during tissue homogenization. The MU-P reporter system allows for simultaneous and independent quantification of encapsulated (MU-P) and free (MU) drug by fluorescence. To increase the sensitivity of this method, we developed an HPLC approach for quantification of MU, MU-P, and MU-G, the major MU metabolite, in homogenized tissues (Figure 1, Figure 5A). An internal standard, 7-hydroxycoumarin (Std), was included to determine the tissue extraction efficiency and monitor the resolution and accuracy of the column. MU, MU-P, MU-G and Std were all readily quantifiable by HPLC in liver, spleen and kidney tissues at both 3 and 48 hours post injection of MU-P loaded liposomes with a detection limit of ~100 ng/mL (Figure 5A, Supplementary Figure 4). To further validate this approach, we compare HPLC and fluorescence measurements of MU and MU-P in serum samples and determine that they provide equivalent results (Supplementary Figure 5).

The encapsulated contents primarily distribute to the liver and spleen, a finding in accordance with the extensive literature on liposome biodistribution over the past 40 years. The MU-P signal was higher in the liver than the spleen, while the inverse was true for MU: indicating faster liposome degradation and higher cellular availability in the spleen. As

expected, the MU-G metabolite was the most abundant species in the kidneys (Supplementary Figure 4, Supplementary Table 4) [29].

The biodistribution results corroborate with the results from the pharmacokinetic study, as the most stable formulations in circulation show the highest drug accumulation in tissue. Importantly, tissue accumulation correlated with total MU-P signal in circulation rather than total lipid signal in circulation, which indicates that the stability of the liposome dictates tissue delivery (Supplementary Figure 6). The C_{16} SML offers improved tissue uptake over the C_{16} CPL at both 3 and 48 hours after injection. While the C_{18} SML and C_{18} CPL demonstrate similar delivery at 3 hours (Figure 5B,C, Supplementary Table 4), contents delivered in the C_{18} SML persist in the tissue longer than contents delivered in the C_{18} CPL (Figure 5B,C, Supplementary Table 4). This trend suggests that in addition to being more stable in circulation, the C_{16} and C_{18} SML demonstrate improved persistence in the liver and spleen as compared to CPL formulations. In stark contrast, the C_{20} CPL demonstrate higher delivery than the C_{20} SML, which again mirrors the stability of these formulations in circulation. Both SML and CPL lipids with unsaturated chains show relatively less delivery to both the liver and spleen, but SML provide better delivery than CPL (Figure 5B,C, Supplementary Table 4).

4. Discussion

We have developed a robust and quantitative method for measuring a critical aspect of liposome disposition *in vivo*: cellular availability. Drug release from liposomes over the wrong timescale or in the wrong cellular location can limit efficacy. Allen and colleagues demonstrate that premature doxorubicin release from unstable liposomes in circulation increases toxicity and decreases efficacy [30]. A large database is now published on the role of stability on circulation of a variety of liposome encapsulated drugs and their efficacy [30-33]. As mentioned earlier, the failure of liposome encapsulated cisplatin in the clinic has been attributed to incomplete release of the drug from the carrier at the tumor site [34]; we think that both the chemistry of the drug and the stability of the liposome contribute to this limitation. The cellular availability of MU-P adds new information concerning the release of contents from the liposome that can be incorporated into pharmacodynamic models to help explain and predict the activity of other liposomal agents.

This report details a method to trace liposomes *in vivo*, and it enables distinct quantification of entrapped and released liposome contents in tissues. While other methods for quantification of liposome contents release exist, their utility is restricted by their complexity [21], sensitivity [20], or narrow applicability [18]. In designing this approach, we searched for a tracer compound that would meet the following criteria: (1) safe at high doses, (2) highly fluorescent, (3) fast excretion when released into extracellular fluids, and (4) undergoes a conformational change when released from the liposome. MU-P fulfills all four of these criteria. MU is extremely safe both in mice and humans[29]. In mice, the maximum tolerated dose for MU-P administered intravenously was greater than 500 mg/kg (data not shown). MU-P released from the liposome is either cleared from circulation or rapidly converted to MU. When tissue samples are isolated and homogenized in the presence of a phosphatase inhibitor, the MU-P that is detected is entrapped in the liposome.

We use this method to explore how liposome composition influences the cellular availability of MU-P after intravenous administration of MU-P liposomes. We find that liposomes composed of SML, in which the cholesterol is covalently anchored in the bilayer, release MU-P more slowly than traditional liposomes containing free cholesterol. This result suggests that SML release contents over a longer timescale and may be useful in the delivery of water soluble drugs that require a sustained duration to exhibit a maximal therapeutic effect. This sustained release can be tuned by adjusting the length of the acyl chain at the 1 position of the SML. Interestingly, SML and CPL show similar pharmacokinetic profiles but different biodistribution and degradation patterns in tissues. This result suggests that cholesterol transfer is an important component of liposome degradation in the liver and spleen.

Our approach has broad applicability *in vitro* and *in vivo.* The *in vitro* leakage experiments clearly demonstrate that MU-P is stably encapsulated in a range of lipid formulations. In contrast to CF, MU-P can be used to probe the stability of formulations with short saturated or unsaturated chains. More important, however, is the *in vivo* utility of this method. We show that it is possible to continuously monitor the fraction of intact liposomes in a given tissue; this is a measurement not easily determined using other approaches.

Supplementary Material

Refer to Web version on PubMed Central for supplementary material.

Acknowledgments

We would like to thank Dr. Charles Noble for his guidance with the HPLC assays and Dr. Saul Kivimäe for help with animal experiments. We would also like to thank Jonathan Sockolosky and Dr. J. P. Michael Motion for their discussions on the manuscript. This work was supported by R01 GM061851.

References

[1]. Zamboni WC, Gervais AC, Egorin MJ, Schellens JHM, Zuhowski EG, Pluim D, et al. Systemic and tumor disposition of platinum after administration of cisplatin or STEALTH liposomal-cisplatin formulations (SPI-077 and SPI-077 B103) in a preclinical tumor model of melanoma. Cancer Chemother. Pharmacol. 2004; 53:329–336. [PubMed: 14673619]

[2]. Drummond DC, Noble CO, Hayes ME, Park JW, Kirpotin DB. Pharmacokinetics and in vivo drug release rates in liposomal nanocarrier development. J Pharm Sci. 2008; 97:4696–4740. [PubMed: 18351638]

[3]. Rahman Y-E, Wright BJ. Liposomes containing chelating agents. Cellular penetration and a possible mechanism of metal removal. J. Cell Biol. 1975; 65:112–122. [PubMed: 805148]

[4]. Thomas AM, Kapanen AI, Hare JI, Ramsay E, Edwards K, Karlsson G, et al. Development of a liposomal nanoparticle formulation of 5-fluorouracil for parenteral administration: formulation design, pharmacokinetics and efficacy. J Control Release. 2011; 150:212–219. [PubMed: 21094191]

[5]. Harrington KJ, Mohammadtaghi S, Uster PS, Glass D, Peters AM, Vile RG, et al. Effective targeting of solid tumors in patients with locally advanced cancers by radiolabeled pegylated liposomes. Clin Cancer Res. 2001; 7:243–254. [PubMed: 11234875]

[6]. Rudolph AS, Klipper RW, Goins B, Phillips WT. In vivo biodistribution of a radiolabeled blood substitute: 99mTc-labeled liposome-encapsulated hemoglobin in an anesthetized rabbit. Proc Natl Acad Sci U S A. 1991; 88:10976–10980. [PubMed: 1961766]

[7]. Gabizon A, Hliberty J, Straubinger RM, Price DC, Papahadjopoulos D. An Improved Method for in Vivo Tracing and Imaging of Liposomes Using a Gallium 67-Deferoxamine Complex. J Liposome Res. 1988; 1:123–135.

[8]. Abra RM, Schreier H, Szoka FC. The use of a new radioactive-iodine labeled lipid marker to follow in vivo disposition of liposomes: comparison with an encapsulated aqueous space marker. Res. Commun. Chem. Pathol. Pharmacol. 1982; 37:199–213. [PubMed: 7134628]

[9]. Claassen E. Post-formation fluorescent labelling of liposomal membranes. In vivo detection, localisation and kinetics. J. Immunol. Methods. 1992; 147:231–240. [PubMed: 1548405]

[10]. Struck DK, Hoekstra D, Pagano RE. Use of resonance energy transfer to monitor membrane fusion. Biochemistry. 1981; 20:4093–4099. [PubMed: 7284312]

[11]. Damen J, Regts J, Scherphof G. Transfer and exchange of phospholipid between small unilamellar liposomes and rat plasma high density lipoproteins. Dependence on cholesterol content and phospholipid composition. Biochim Biophys Acta. 1981; 665:538–545. [PubMed: 7295749]

[12]. Weinstein JN, Yoshikami S, Henkart P, Blumenthal R, Hagins WA. Liposome-cell interaction: transfer and intracellular release of a trapped fluorescent marker. Science. 1977; 195:489–492. [PubMed: 835007]

[13]. Perche F, Patel NR, Torchilin VP. Accumulation and toxicity of antibody-targeted doxorubicin-loaded PEG–PE micelles in ovarian cancer cell spheroid model. J Control Release. 2012; 164:95–102. [PubMed: 22974689]

[14]. Chaudhuri, T. Roy; Arnold, RD.; Yang, J.; Turowski, SG.; Qu, Y.; Spernyak, JA., et al. Mechanisms of tumor vascular priming by a nanoparticulate doxorubicin formulation. Pharm Res. 2012; 29:3312–3324. [PubMed: 22798260]

[15]. Wu NZ, Braun RD, Gaber MH, Lin GM, Ong ET, Shan S, et al. Simultaneous measurement of liposome extravasation and content release in tumors. Microcirculation. 1997; 4:83–101. [PubMed: 9110286]

[16]. Ellens H, Bentz J, Szoka FC. Proton-and calcium-induced fusion and destabilization of liposomes. Biochemistry. 1985; 24:3099–3106. [PubMed: 4027232]

[17]. Schroeder A, Honen R, Turjeman K, Gabizon A, Kost J, Barenholz Y. Ultrasound triggered release of cisplatin from liposomes in murine tumors. J Control Release. 2009; 137:63–68. [PubMed: 19303426]

[18]. Laginha KM, Verwoert S, Charrois GJR, Allen TM. Determination of doxorubicin levels in whole tumor and tumor nuclei in murine breast cancer tumors. Clin Cancer Res. 2005; 11:6944–6949. [PubMed: 16203786]

[19]. Tippayamontri T, Kotb R, Paquette B, Sanche L. Cellular uptake and cytoplasm / DNA distribution of cisplatin and oxaliplatin and their liposomal formulation in human colorectal cancer cell HCT116. Invest New Drugs. 2011; 29:1321–1327. [PubMed: 20658169]

[20]. Mauk MR, Gamble RC, Baldeschwieler JD. Targeting of lipid vesicles: specificity of carbohydrate receptor analogues for leukocytes in mice. Proc Natl Acad Sci U S A. 1980; 77:4430–4434. [PubMed: 6933495]

[21]. Szoka FC Jr. Jones CS. [14] Uptake of liposome-encapsulated agents. Meth Enzymol. 1987; 149:143–147. [PubMed: 3121982]

[22]. Fernley HN, Walker PG. Kinetic behaviour of calf-intestinal alkaline phosphatase with 4-methylumbelliferyl phosphate. Biochem. J. 1965; 97:95–103. [PubMed: 16749130]

[23]. Huang Z, Jaafari MR, Szoka FC. Disterolphospholipids: nonexchangeable lipids and their application to liposomal drug delivery. Angew Chem Int Ed Engl. 2009; 48:4146–4149. [PubMed: 19425026]

[24]. Huang Z, Szoka FC. Sterol-Modified Phospholipids: Cholesterol and Phospholipid Chimeras with Improved Biomembrane Properties. J Am Chem Soc. 2008; 130:15702–15712. [PubMed: 18950160]

[25]. Vest R, Wallis R, Jensen LB, Haws AC, Callister J, Brimhall B, et al. Use of steady-state laurdan fluorescence to detect changes in liquid ordered phases in human erythrocyte membranes. J. Membr. Biol. 2006; 211:15–25. [PubMed: 16988865]

[26]. van Kempen GM, Jansen GS. Quantitative determination of phenolsulfotransferase using 4-methylumbelliferone. Anal. Biochem. 1972; 46:438–442. [PubMed: 5024616]

[27]. Denu JM, Lohse DL, Vijayalakshmi J, Saper MA, Dixon JE. Visualization of intermediate and transition-state structures in protein-tyrosine phosphatase catalysis. Proc Natl Acad Sci U S A. 1996; 93:2493–2498. [PubMed: 8637902]

[28]. Lentz BR. Use of fluorescent probes to monitor molecular order and motions within liposome bilayers. Chem Phys Lipids. 1993; 64:99–116. [PubMed: 8242843]

[29]. Garrett ER, Venitz J, Eberst K, Cerda JJ. Pharmacokinetics and bioavailabilities of hymecromone in human volunteers. Biopharm Drug Dispos. 1993; 14:13–39. [PubMed: 8427942]

[30]. Allen TM, Mumbengegwi DR, Charrois GJR. Anti-CD19-targeted liposomal doxorubicin improves the therapeutic efficacy in murine B-cell lymphoma and ameliorates the toxicity of liposomes with varying drug release rates. Clin Cancer Res. 2005; 11:3567–3573. [PubMed: 15867261]

[31]. Drummond DC, Noble CO, Guo Z, Hayes ME, Connolly-Ingram C, Gabriel BS, et al. Development of a highly stable and targetable nanoliposomal formulation of topotecan. J Control Release. 2010; 141:13–21. [PubMed: 19686789]

[32]. Alabi CA, Love KT, Sahay G, Yin H, Luly KM, Langer R, et al. Multiparametric approach for the evaluation of lipid nanoparticles for siRNA delivery. Proc Natl Acad Sci USA. 2013; 110:12881–12886. [PubMed: 23882076]

[33]. Mayer LD, Tai LC, Ko DS, Masin D, Ginsberg RS, Cullis PR, et al. Influence of vesicle size, lipid composition, and drug-to-lipid ratio on the biological activity of liposomal doxorubicin in mice. Cancer Res. 1989; 49:5922–5930. [PubMed: 2790807]

[34]. Kim ES, Lu C, Khuri FR, Tonda M, Glisson BS, Liu D, et al. A phase II study of STEALTH cisplatin (SPI-77) in patients with advanced non-small cell lung cancer. Lung Cancer. 2001; 34:427–432. [PubMed: 11714540]

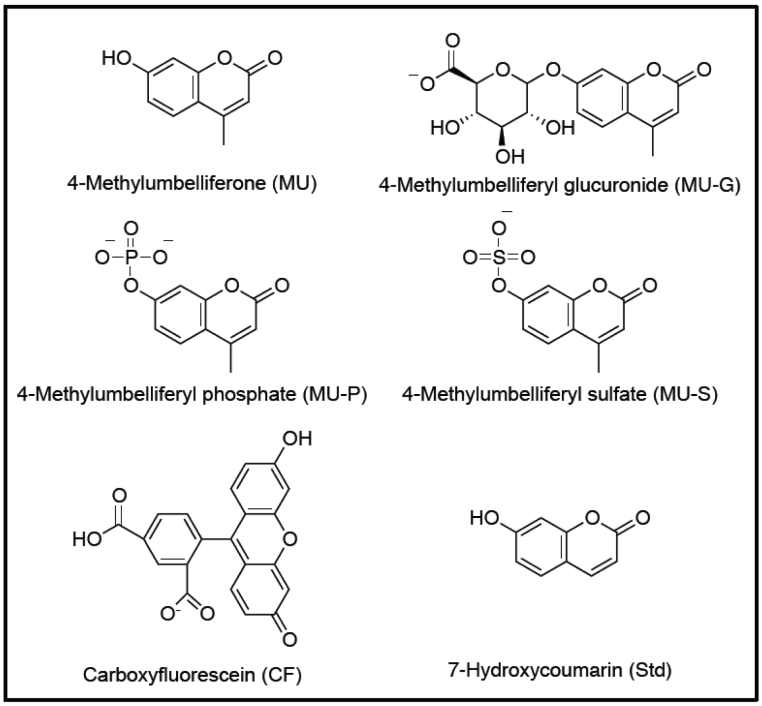

Figure 1. Relevant Structures

Structures of 4-methylumbelliferone (MU), MU metabolite 4-methylumbelliferyl glucuronide (MU-G), MU prodrugs 4-methylumbelliferyl phosphate (MU-P) and 4-methylumbelliferyl sulfate (MU-S), carboxyfluorescein (CF), and HPLC standard 7-hydroxycoumarin (Std).

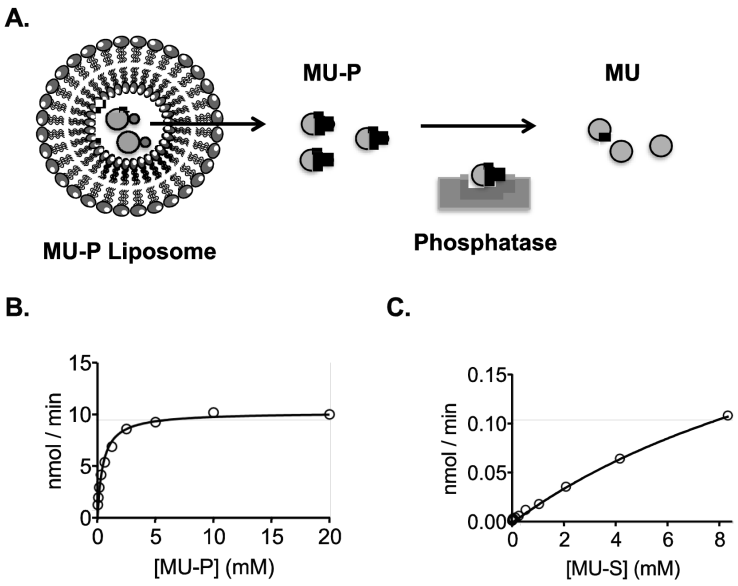

Figure 2. MU-P Reporter System

(A) MU-P is encapsulated in liposomes. Upon leakage from liposomes, MU-P is rapidly converted to MU by endogenous phosphatases. (B,C) Michaelis-Menten kinetics of MU-P and MU-S conversion in mouse serum.

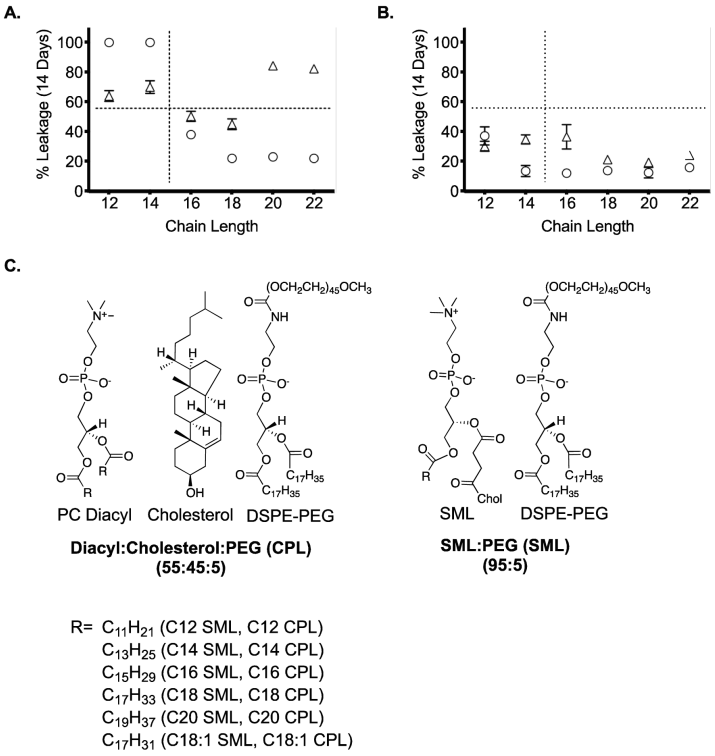

Figure 3. Effects of Acyl Chain Length, Saturation, and Liposome Composition on Membrane Stability

CF (A) or MU-P (B) was passively encapsulated in (C) a range of CPL (○) or SML (Δ). Molar ratios of liposome formulations are given. Liposomes were incubated in HBS containing 30% serum. The percent of MU-P leaked from liposomes after 14 days is shown.

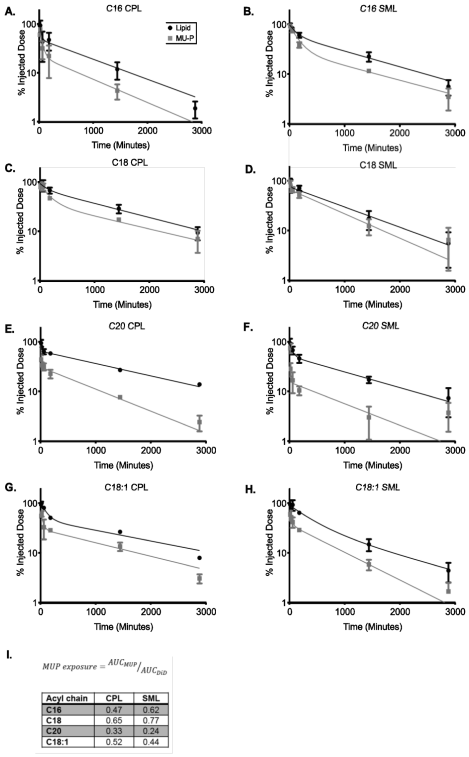

Acyl chain	CPL	SML
C16	0.47	0.62
C18	0.65	0.77
C20	0.33	0.24
C18:1	0.52	0.44

Figure 4. Evaluation of SML and CPL Stability in Circulation by Fluorescence

(A-H) MU-P, MU and DiD signals were measured in serum samples by fluorescence. The MU-P and DiD data is fit to a two-compartment model. MU was undetectable in serum at all time points. (I) The ratio of (AUC_{MUP}/AUC_{DiD}) for each formulation is shown.

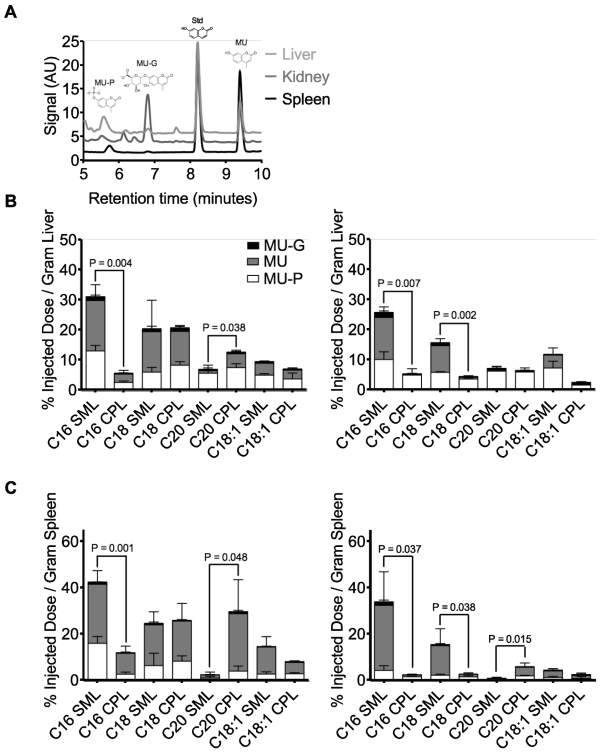

Figure 5. SML Alter Delivery to the Liver and Spleen

(A) HPLC trace from the liver, spleen, and kidney of a mouse injected with liposomal MU-P. Percent of injected dose in the (B) liver and (C) spleen at 3 hours (left) and 48 hours (right) after administration. MU, MU-P and MU-G levels are shown and sum to the total amount of MU equivalents in the tissue.